



## Development of Highly Productive Nickel-Sodium Phenoxyphosphine Ethylene Polymerization Catalysts and Their Reaction Temperature Profiles

Journal:	<i>Polymer Chemistry</i>
Manuscript ID	PY-COM-04-2019-000610.R1
Article Type:	Communication
Date Submitted by the Author:	29-May-2019
Complete List of Authors:	Tran, Thi; University of Houston, Chemistry Nguyen, Yennie H.; University of Houston, Chemistry Do, Loi; University of Houston, Chemistry

## Development of Highly Productive Nickel-Sodium Phenoxyphosphine Ethylene Polymerization Catalysts and Their Reaction Temperature Profiles

Received 00th January 20xx,  
Accepted 00th January 20xx

DOI: 10.1039/x0xx00000x

Thi V. Tran, Yennie H. Nguyen, Loi H. Do\*

www.rsc.org/

We have successfully applied a pendent Lewis acid design strategy to enhance the ethylene polymerization rates of nickel phenoxyphosphine catalysts. Our heterobimetallic complex is among one of the most productive coordination insertion catalysts reported to date for nickel. Due to its tendency to generate large reaction exotherms, it is necessary to apply continuous temperature control and low catalyst loading to achieve optimal efficiency.

Late transition metal complexes are widely investigated as olefin polymerization catalysts because they have better functional monomer compatibility and greater tolerance of polar impurities/solvents compared to early transition metal complexes.<sup>1-6</sup> An extensive assortment of nickel catalysts (e.g. **Ni1-Ni9** in Chart 1) with diverse ethylene polymerization behaviour has now been reported.<sup>7-15</sup> Some of their common limitations, however, are that they can exhibit low catalyst activity, produce short chain oligomers/polymers, and have poor control over polymer microstructures.

Research in our group has been focusing on new strategies to enhance the capabilities of late transition metal olefin polymerization catalysts. We had shown previously that when nickel phenoxyimine<sup>16-18</sup> or palladium phosphine phosphate ester catalysts<sup>19,20</sup> were paired with secondary Lewis acids, their reactivity could be significantly bolstered and/or altered. In the current work, we demonstrate that the presence of sodium ions could also dramatically accelerate the ethylene polymerization rates of nickel phenoxyphosphine catalysts.<sup>13,21</sup> Under optimal reaction conditions, our nickel-sodium complexes could rival some of the best nickel olefin polymerization catalysts that have been reported. This study illustrates the versatility of our catalyst design strategy and suggests that new classes of advanced olefin polymerization catalysts might be accessible using this approach.

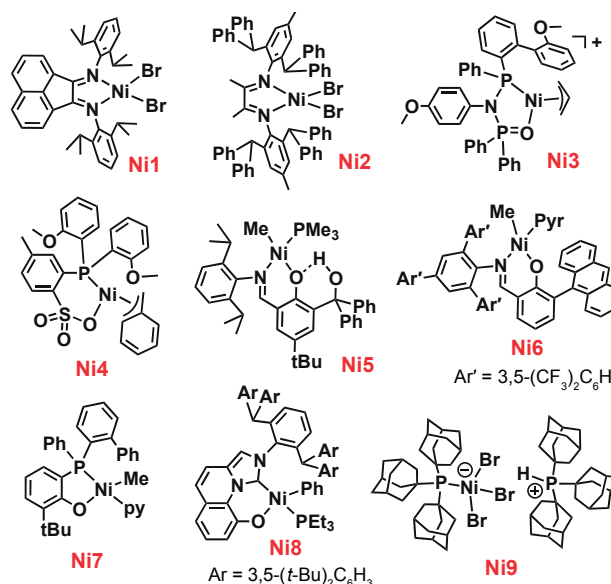
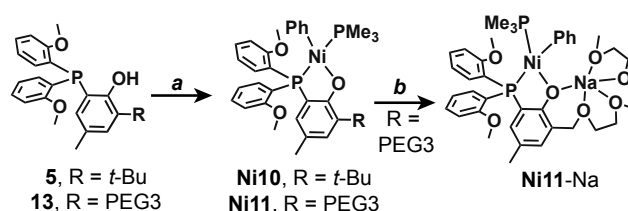


**Chart 1.** Nickel ethylene polymerization catalysts reported in the literature.



**Scheme 1.** Synthesis of nickel phenoxyphosphine complexes. Step a: 1) NaH, THF, 2) NiPhBr(PMe<sub>3</sub>)<sub>2</sub>; Step b: NaBAR<sub>4</sub>. PEG3 = CH<sub>2</sub>(OCH<sub>2</sub>CH<sub>2</sub>)<sub>3</sub>OCH<sub>3</sub>.

To enable the incorporation of pendent alkali ions to nickel phenoxyphosphine complexes, we attached polyethylene glycol (PEG) chains to the *ortho* position of the phenolate ring (Scheme 1).<sup>16</sup> The PEGylated ligand **13** was synthesized using a multi-step procedure outlined in Scheme S1. Metallation of **13**

Department of Chemistry, University of Houston,  
4800 Calhoun Rd., Houston, TX 77004, USA  
Email: loido@uh.edu

Electronic Supplementary Information (ESI) available: procedures, titration data, polymerization, NMR characterization. See DOI: 10.1039/x0xx00000x

was achieved by deprotonation using sodium hydride, followed by the addition of  $\text{NiPhBr}(\text{PMe}_3)_2$  to provide complex **Ni11** (Scheme 1). For control studies, we also prepared the conventional nickel phenoxyphosphine complex featuring *ortho tert*-butyl groups (**Ni10**).<sup>21</sup>

Because of its favourable properties, we focused our investigations on sodium as the secondary metal.<sup>16,17</sup> To determine whether  $\text{Na}^+$  can coordinate to **Ni11**, we carried out metal titration studies by UV-visible absorption spectroscopy. We observed that when aliquots of  $\text{NaBAR}_4^{\text{F}_4}$  (where  $\text{BAR}_4^{\text{F}_4}^- = \text{tetrakis}(3,5\text{-bis}(\text{trifluoromethyl})\text{phenyl})\text{borate}$ )<sup>22</sup> were added to a solution of **Ni11** in  $\text{Et}_2\text{O}$ , the optical band at  $\sim 370$  nm gradually decreased while the optical band at  $\sim 330$  nm increased (Figure S2). The appearance of isosbestic points at 326 and 359 nm suggests that the addition of  $\text{Na}^+$  to **Ni11** led to the formation of a new optically active species. The optimal Ni:Na binding stoichiometry was determined to be 1:1 by Job Plot studies (Figure S3).<sup>23</sup> To obtain structural characterization, we grew single crystals of the nickel-sodium complex by layering pentane over a toluene/ $\text{Et}_2\text{O}$  solution of **Ni11** and  $\text{NaBAR}_4^{\text{F}_4}$  (1:1). Its X-ray structure revealed a heterobimetallic complex with the composition  $\text{NiNa}(\text{phenoxyphosphine-PEG})\text{Ph}(\text{PMe}_3)$  (**Ni11-Na**, Figure 1). The nickel centre is four-coordinate, in which the phenyl group is coordinated *trans* relative to the phosphorus donor P1. Presumably, this orientation is preferred due to metal- $\pi$  interactions between the adjacent sodium ion and phenyl ring (C30–C31). The sodium is ligated by four PEG oxygen atoms and a phenolate donor. Although complex **Ni11** itself could not be crystallized for X-ray diffraction analysis, the structure of the related mononickel **Ni10** showed that the nickel centre is square planar but the coordinated phenyl group is *cis* relative to P1 (Figure S41). Interestingly, when a solution of **Ni10** in  $\text{Et}_2\text{O}$  was treated with up to 4 equiv. of  $\text{NaBAR}_4^{\text{F}_4}$ , no UV-visible absorption changes were observed (Figure S1), indicating that there are no coordination interactions between complex **Ni10** and  $\text{Na}^+$ .

With our nickel complexes in hand, we tested their catalytic performance by first activation using  $\text{Ni}(\text{COD})_2$  (COD = 1,5-cyclooctadiene) and then exposure to 450 psi of ethylene at 30°C for 1 h in toluene. To minimize catalyst thermal decomposition, the polymerization studies in Table 1 were performed using a low catalyst concentration of 5  $\mu\text{M}$  and with manual external cooling to maintain the desired reaction temperature. Under these conditions, complex **Ni10** produced linear polyethylene (PE) with an activity of  $2.12 \times 10^3$   $\text{kg/mol} \cdot \text{h}$  (Table 1, entry 1). The addition of  $\text{NaBAR}_4^{\text{F}_4}$  (entry 2), or  $\text{NaBAR}_4^{\text{F}_4}/15\text{-crown-4}$  ether (1:1, entry 3) to **Ni10** had negligible effects on polymerization, which further supports our observation that  $\text{Na}^+$  does not bind to **Ni10**.

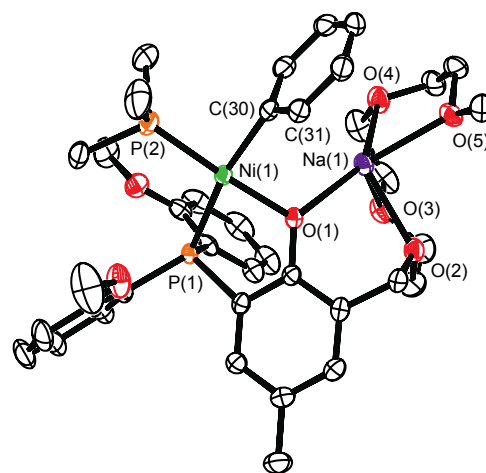


**Figure 1.** X-ray structure of complex **Ni11-Na** (ORTEP view, displacement ellipsoids drawn at 50% probability level). Hydrogen atoms and the  $\text{BAR}_4^{\text{F}_4}^-$  anion have been omitted for clarity.

**Table 1.** Ethylene Polymerization Data<sup>a</sup>

Entry	Complex	Pressure (psi)	Time (h)	Initial Temp. (°C)	Activity (kg/mol·h)
1	<b>Ni10</b>	450	1	30	2120
2	<b>Ni10/Na<sup>+</sup></b>	450	1	30	1880
3	<b>Ni10/Na<sup>+</sup>/15-crown-5<sup>b</sup></b>	450	1	30	1920
4	<b>Ni11</b>	450	1	30	0
5	<b>Ni11-Na</b>	150	1	20	3780
6	<b>Ni11-Na</b>	300	1	20	8840
7	<b>Ni11-Na</b>	450	1	20	10800
8	<b>Ni11-Na</b>	450	0.5	30	25300
9	<b>Ni11-Na</b>	450	1	30	18100
10	<b>Ni11-Na</b>	450	2	30	15080
11	<b>Ni11-Na</b>	450	1	20	10800
12	<b>Ni11-Na</b>	450	1	40	14700
13	<b>Ni11-Na</b>	450	1	50	13000
14	<b>Ni11-Na</b>	450	1	60	9380

<sup>a</sup>Conditions: Ni catalyst (0.5  $\mu\text{mol}$ ),  $\text{NaBAR}_4^{\text{F}_4}$  (1  $\mu\text{mol}$ , if any),  $\text{Ni}(\text{COD})_2$  (4  $\mu\text{mol}$ ), 100 mL toluene. Temperature was controlled by manual external cooling when necessary to ensure that the reaction temperature does not exceed greater than 5°C from the starting temperature. More detailed polymerization data, including molecular weight, are provided in the Supporting Information. <sup>b</sup>The 15-crown-5 ether amount used was 1  $\mu\text{mol}$ .

Surprisingly, when **Ni11** was tested under the same conditions as above, no polyethylene was obtained (Table 1, entry 3). We hypothesized that the free PEG chain in **Ni11** could self-inhibit by occupying open coordination sites at the nickel centre. However, when  $\text{NaBAR}_4^{\text{F}_4}$  was added to **Ni11**, the resulting nickel-sodium **Ni11-Na** showed a remarkably activity of  $1.81 \times 10^4$   $\text{kg/mol} \cdot \text{h}$  (entry 9), which is a  $\sim 8.5\times$  increase in comparison to that of **Ni10**. The PE produced by **Ni10** and **Ni11-Na** both have linear microstructures, low molecular weight ( $M_n = \sim 10^3$ ), and narrow polydispersity ( $M_w/M_n = < 2.0$ ), which is typical for this class of catalysts (Table S4).<sup>13,21</sup> The catalyst enhancing effects of the sodium cation were observed in previous investigations of nickel phenoxyimine<sup>16-18</sup> and palladium phosphine phosphate ester catalysts<sup>19,20</sup>. Although

studies are currently ongoing to understand the origin of this Lewis acid effect, we tentatively attribute it to both electrophilic activation of the nickel centre as well as increased steric protection by the sodium-PEG structure.

A comparison with several different nickel systems reported in the literature indicates that **Ni11**-Na is among one of the most *productive* (Table S10, note: different studies used different polymerization conditions to achieve optimal results).<sup>7-15</sup> Although the nickel diimine (**Ni1**)<sup>7</sup> and nickel tris(adamantyl)phosphine (**Ni9**)<sup>15</sup> complexes could achieve extraordinarily high activity, our **Ni11**-Na complex gave the highest turnover number (TON). For example, the TON for **Ni11**-Na was  $646 \times 10^3$ , whereas the TON for **Ni1** and **Ni9** were  $400 \times 10^3$  and  $216 \times 10^3$ , respectively. Interestingly, catalysts **Ni1** and **Ni9** furnished PE with significantly higher molecular weights ( $M_n \geq 10^5$ ) than that of **Ni11**-Na ( $M_n \approx 10^3$ ). However, it is well established that higher  $M_n$  polymers could be obtained by increasing the steric bulk of the catalyst structure.<sup>24,25</sup>

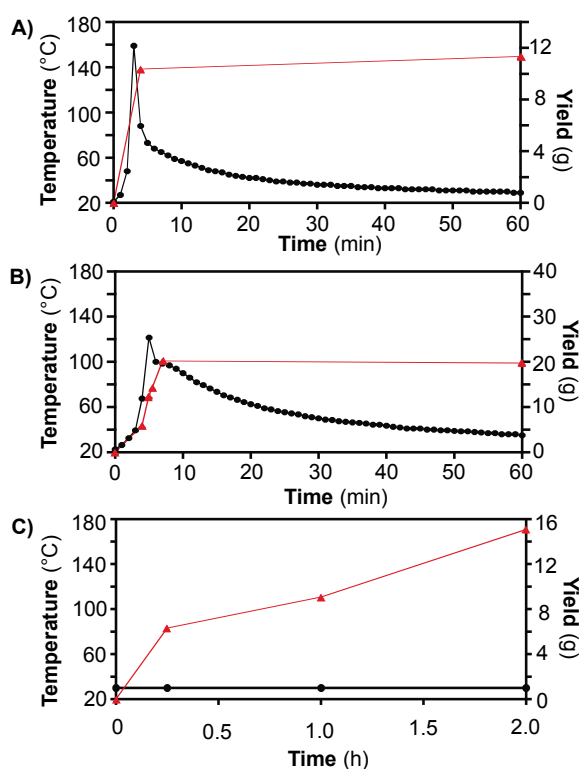


**Figure 2.** Plots showing the reaction temperatures (black dots) and polymer yields (red triangles) by the **Ni11**-Na complex at 100  $\mu\text{M}$  (A) and 50  $\mu\text{M}$  (B) catalyst concentrations. When external temperature control was applied (C), the **Ni11**-Na (5  $\mu\text{M}$ ) catalyst gave increasing amounts of PE up to the 2 h polymerization time. All reactions were performed under 450 psi of ethylene.

To investigate the polymerization behaviour of **Ni11**-Na further, we evaluated its reactivity as a function of pressure, time, and temperature. We found that when the ethylene pressure was increased from 150  $\rightarrow$  300  $\rightarrow$  450 psi (Table 1, entries 4-6), the catalyst activity also increased. The

approximately linear correlation between pressure and polymerization rate suggests that the reaction is first-order in ethylene. At 150 psi and 20°C (Table S4), **Ni11**-Na showed relatively constant activity (average =  $3.3 \times 10^3$  kg/mol·h) up to 3.0 h. However, at 450 psi and 30°C (Table 1), the activity gradually decreased from  $2.5 \times 10^4$  (entry 8) to  $1.5 \times 10^4$  kg/mol·h (entry 10) over the course of 2 h, which could be indicative of either catalyst decomposition or mass transport limitations. In the latter case, it has been shown that precipitation of large amounts of polymer inside a reactor could dramatically slow down the polymerization process.<sup>8,15</sup> Finally, when we performed polymerizations at different temperatures (20 to 60°C, entries 8 and 10-13), we observed that the optimal temperature was 30°C. For some reactions, the initial temperature spiked abruptly and was difficult to control. This large exotherm only occurred when the **Ni11**-Na complex was used. Polymerizations using the monometallic **Ni10** and **Ni11** complexes did not generate any additional heat.

To evaluate the thermal stability of the **Ni11**-Na complex, we measured the reaction temperature and polymer yields as a function of time. When a 100  $\mu\text{M}$  toluene solution of the nickel-sodium catalyst was treated with  $\text{Ni}(\text{COD})_2$  and then exposed to 450 psi of ethylene, the reaction temperature rose from 20 to 159°C in 4 min (Figure 2A). After this initial temperature increase, the solution cooled slowly back down to  $\sim 20^\circ\text{C}$  after 60 min. Interestingly, when the product yields were determined at 4 and 60 min, similar amounts of polymer were obtained ( $\sim 10.4$  and  $\sim 11.3$  g, respectively). This result suggests that the **Ni11**-Na catalyst was deactivated shortly after  $\sim 4$  min. When the **Ni11**-Na concentration was lowered to 50  $\mu\text{M}$ , the maximum reaction temperature was observed to be 122°C after 5 min (Figure 2B). The rate of polymer formation remained relatively constant from 0-7 min but then dropped precipitously thereafter. In contrast, when the reactor temperature was maintained at 30°C during a 2 h trial, and using a **Ni11**-Na concentration of 5  $\mu\text{M}$ , the amount of PE produced increased steadily over time (Figure 2C), suggesting that there was minimal catalyst deactivation during polymerization.

In summary, we have synthesized a new class of nickel phenoxyphosphine complexes featuring PEG side arms that can chelate secondary sodium ions. We have found that the **Ni11**-Na complexes are remarkably efficient catalysts for ethylene polymerization, demonstrating once again that the use of pendent Lewis acids is an effective strategy to enhance catalyst performance.<sup>16,19</sup> This work also illustrates the importance of conducting detailed temperature studies to optimize polymerization processes. Although there are numerous reports that highly active catalysts can exhibit large exotherms,<sup>8,15,18,26</sup> seldom are their reaction temperature profiles provided. This information is useful because it allows us to predict what are the best reaction conditions to use for a given catalyst. For example, by operating just below the temperature at which **Ni11**-Na decomposes, we were able to achieve one of the highest TON reported for a nickel catalyst. Although it is standard practice to disclose only the reactor temperature at the start of a reaction, we recommend also

providing temperature data for the full polymerization time to allow us to gain insights into a catalyst's true thermal stability.

(26) Zhang, Y.-P.; Li, W.-W.; Li, B.-X.; Mu, H.-L.; Li, Y.-S. *Dalton Trans.* **2015**, *44*, 7382-7394.

### Conflicts of interest

There are no conflicts to declare.

### Acknowledgements

We thank the Welch Foundation (Grant No. E-1894) and National Science Foundation (Grant No. CHE-1750411) for their generous support of this research.

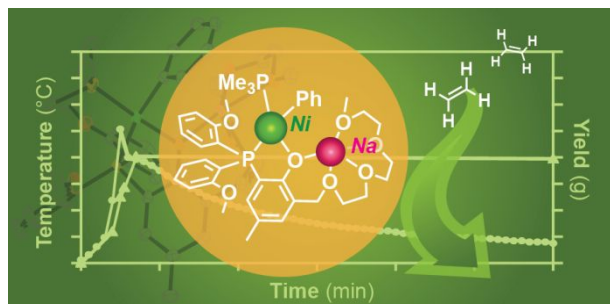
### References

- (1) Ittel, S. D.; Johnson, L. K.; Brookhart, M. *Chem. Rev.* **2000**, *100*, 1169-1203.
- (2) Nakamura, A.; Anselment, T. M. J.; Claverie, J.; Goodall, B.; Jordan, R. F.; Mecking, S.; Rieger, B.; Sen, A.; van Leeuwen, P. W. N. M.; Nozaki, K. *Acc. Chem. Res.* **2013**, *46*, 1438-1449.
- (3) Carrow, B. P.; Nozaki, K. *Macromolecules* **2014**, *47*, 2541-2555.
- (4) Chen, Z.; Brookhart, M. *Acc. Chem. Res.* **2018**, *51*, 1831-1839.
- (5) Tan, C.; Chen, C. *Angew. Chem. Int. Ed.* **2019**, *58*, 7192-7200.
- (6) Chen, C. *Nat. Rev. Chem.* **2018**, *2*, 6-14.
- (7) Gates, D. P.; Svejda, S. A.; Oñate, E.; Killian, C. M.; Johnson, L. K.; White, P. S.; Brookhart, M. *Macromolecules* **2000**, *33*, 2320-2334.
- (8) Rhinehart, J. L.; Brown, L. A.; Long, B. K. *J. Am. Chem. Soc.* **2013**, *135*, 16316-16319.
- (9) Chen, M.; Chen, C. *Angew. Chem. Int. Ed.* **2018**, *57*, 3094-3098.
- (10) Zhou, X.; Bontemps, S.; Jordan, R. F. *Organometallics* **2008**, *27*, 4821-4824.
- (11) Delferro, M.; McInnis, J. P.; Marks, T. J. *Organometallics* **2010**, *29*, 5040-5049.
- (12) Kenyon, P.; Wörner, M.; Mecking, S. *J. Am. Chem. Soc.* **2018**, *140*, 6685-6689.
- (13) Zhang, Y.; Mu, H.; Pan, L.; Wang, X.; Li, Y. *ACS Catal.* **2018**, *8*, 5963-5976.
- (14) Noda, S.; Kochi, T.; Nozaki, K. *Organometallics* **2009**, *28*, 656-658.
- (15) Kocen, A.; Brookhart, M.; Daugulis, O. *Nat. Commun.* **2019**, *10*, 438.
- (16) Cai, Z.; Xiao, D.; Do, L. H. *J. Am. Chem. Soc.* **2015**, *137*, 15501-15510.
- (17) Cai, Z.; Do, L. H. *Organometallics* **2017**, *36*, 4691-4698.
- (18) Younkin, T. R.; Connor, E. F.; Henderson, J. I.; Friedrich, S. K.; Grubbs, R. H.; Bansleben, D. A. *Science* **2000**, *287*, 460-462.
- (19) Cai, Z.; Do, L. H. *Organometallics* **2018**, *37*, 3874-3882.
- (20) Contrella, N. D.; Sampson, J. R.; Jordan, R. F. *Organometallics* **2014**, *33*, 3546-3555.
- (21) Xin, B. S.; Sato, N.; Tanna, A.; Oishi, Y.; Konishi, Y.; Shimizu, F. *J. Am. Chem. Soc.* **2017**, *139*, 3611-3614.
- (22) Brookhart, M.; Grant, B.; Volpe, A. F., Jr. *Organometallics* **1992**, *11*, 3920-3922.
- (23) Hirose, K. *J. Incl. Phenom. Marocycl. Chem.* **2001**, *39*, 193-209.
- (24) Chen, Z.; Mesgar, M.; White, P. S.; Daugulis, O.; Brookhart, M. *ACS Catal.* **2015**, *5*, 631-636.
- (25) Dai, S.; Zhou, S.; Zhang, W.; Chen, C. *Macromolecules* **2016**, *49*, 8855-8862.

## Journal Name

## COMMUNICATION

## Table of Contents



Heterobimetallic nickel-sodium phenoxyphosphine complexes were found to be among one of the most efficient late metal catalysts for ethylene polymerization.